

Discrete dark matter with light Dirac neutrinos

Debasish Borah,^{1,*} Pritam Das,^{2,†} Biswajit Karmakar,^{3,‡} and Satyabrata Mahapatra^{4,§}

¹*Department of Physics, Indian Institute of Technology, Guwahati, Assam 781039, India*

²*Department of Physics, Salbari College, Baksa, Assam 781318, India*

³*Institute of Physics, University of Silesia, Katowice, Poland*

⁴*Department of Physics and Institute of Basic Science,
Sungkyunkwan University, Suwon 16419, Korea*

Abstract

We propose a new realisation of light Dirac neutrino mass and dark matter (DM) within the framework of a non-Abelian discrete flavour symmetry A_4 . In addition to A_4 , we also consider a Z_2 and an unbroken global lepton number symmetry $U(1)_L$ to keep unwanted terms away while guaranteeing the Dirac nature of light neutrinos. The field content, their transformations and flavon vacuum alignments are chosen in such a way that the type-I Dirac seesaw generates only one light Dirac neutrino mass while the other two masses arise from scotogenic contributions at one-loop. The symmetry breaking of A_4 leaves a remnant Z_2 symmetry responsible for stabilising DM. Dirac nature of light neutrinos introduces additional relativistic degrees of freedom ΔN_{eff} within reach of cosmic microwave background experiments.

*Electronic address: dborah@iitg.ac.in

†Electronic address: prtmDas9@gmail.com

‡Electronic address: biswajit.karmakar@us.edu.pl

§Electronic address: satyabrata@g.skku.edu

I. INTRODUCTION

Origin of light neutrino mass and mixing [1] has been one of the longstanding puzzles in particle physics. While neutrinos remain massless within the framework of the standard model (SM) of particle physics, several beyond standard model (BSM) frameworks have been proposed to explain non-zero neutrino mass and mixing. Canonical seesaw frameworks [2–12] involve inclusion of heavy fields which couple to the SM leptons. These seesaw mechanisms and several of their descendants predict Majorana light neutrino masses which violate lepton number by two units. However, there has been no confirmation about the Majorana nature of light neutrinos with experiments searching for neutrinoless double beta decay (NDBD) continuing to report null results. While null results at NDBD experiments do not necessarily imply Dirac nature of light neutrinos, there has been growing interest in Dirac neutrino models of late. After a few initial attempts in this direction [13–16], several new proposals to realise sub-eV scale Dirac neutrino masses [17–55] have appeared recently. Most of these works, in addition to the inclusion of new fields, also consider new discrete or continuous symmetries in order to forbid unwanted terms in the Lagrangian. In the spirit of Dirac seesaw for light neutrinos, such unwanted terms include the bare mass term of Majorana type for singlet right handed neutrinos (ν_R) and direct coupling of ν_R with the SM lepton and Higgs doublets.

Another observed phenomena which can not be explained in the SM is the presence of dark matter (DM) in the Universe. Its presence is supported by astrophysical observations at different scales [56–58] together with cosmological experiments like PLANCK, WMAP predicting around 26.8% of the present Universe to be made up of DM [1, 59]. While weakly interacting massive particle (WIMP) has been the most widely studied particle DM framework, null results at direct detection experiments [60] have also led to growing interest in alternative scenarios where DM is more feebly coupled to the SM, like the feebly interacting massive particle (FIMP). Recent reviews of WIMP and FIMP can be found in [61] and [62] respectively.

Motivated by this, we propose a new flavour symmetric origin of light Dirac neutrino mass and dark matter in this work. We consider the popular non-Abelian discrete flavour symmetry group of A_4 augmented with an additional discrete Z_2 and global lepton number $U(1)_L$ symmetries. The A_4 flavour symmetry gets spontaneously broken by flavon fields

while generating light Dirac neutrino mass and mixing. For a review of non-Abelian discrete flavour symmetries and their consequences, see Ref. [63–67] and references therein. Unlike popular DM scenarios with additional stabilising symmetries, here we have stable DM by virtue of a remnant Z_2 symmetry naturally emerging from A_4 breaking. Similar scenario for Majorana light neutrino, coined as *discrete dark matter* was proposed in [68] and subsequently explored within different contexts [69–80]. We propose a realisation of this discrete dark matter paradigm with light Dirac neutrinos in a minimal A_4 flavour symmetric setup. We show that neutrino oscillation data can be satisfied after taking tree-level and one-loop contributions to light Dirac neutrino masses. While the model predicts either scalar or fermion DM with the desired relic abundance, light Dirac neutrinos lead to observable ΔN_{eff} at future cosmic microwave background (CMB) experiments like CMB Stage IV (CMB-S4) [81], SPT-3G [82], Simons Observatory [83] and CMB-HD [84].

This paper is organised as follows. In section II, we discuss our model and the origin of light Dirac neutrino mass with stable dark matter. In section III, we discuss the numerical analysis related to neutrino mass and mixing followed by discussion of dark matter, ΔN_{eff} and other detection prospects in section IV, V, VI respectively. Finally, we conclude in section VII.

II. THE MODEL

In this section, we discuss the relevant field content of the model, the field transformations under the chosen symmetries and the particle spectrum. Table I summarises the relevant field content and the corresponding quantum numbers. The SM lepton doublets and right chiral part of Dirac neutrino (ν_R) transform as A_4 singlets while heavy vector-like SM gauge singlet fermions $N_{L,R}$ transform as A_4 triplets. In addition to the SM Higgs H transforming as A_4 singlet, additional scalar doublet η and scalar singlet χ both transforming as A_4 triplets are included. The additional Z_2 symmetry prevents direct coupling of SM lepton doublet, SM Higgs doublet and ν_R . On the other hand, a global unbroken lepton number symmetry $U(1)_L$ prevent Majorana mass terms guaranteeing the Dirac nature of light neutrinos. The Yukawa Lagrangian for charged lepton can be written as

$$-\mathcal{L}_{\text{CL}} \supset Y_e \bar{\ell}_e H e_R + Y_\mu \bar{\ell}_\mu H \mu_R + Y_\tau \bar{\ell}_\tau H \tau_R + \text{h.c.} \quad (1)$$

On the other hand, the neutral fermion Lagrangian is given by

Fields	ℓ_e	ℓ_μ	ℓ_τ	e_R	μ_R	τ_R	$N_{L,R}$	$\nu_{R_{e,\mu,\tau}}$	η	χ	H
$SU(2)$	2	2	2	1	1	1	1	1	2	1	2
A_4	1	1''	1'	1	1''	1'	3	1, 1', 1''	3	3	1
Z_2	1	1	1	1	1	1	1	-1	1	-1	1
$U(1)_L$	1	1	1	1	1	1	1	1	0	0	0

TABLE I: Field contents and transformation under the symmetries of our model.

$$\begin{aligned}
-\mathcal{L}_\nu &\supset y_1 \bar{\ell}_e (N_R \tilde{\eta})_1 + y_2 \bar{\ell}_\mu (N_R \tilde{\eta})_{1''} + y_3 \bar{\ell}_\tau (N_R \tilde{\eta})_{1'} \\
&\quad + M_N (\bar{N}_L N_R)_1 + y'_1 (\bar{N}_L \chi)_1 \nu_{Re} + y'_2 (\bar{N}_L \chi)_{1''} \nu_{R\mu} + y'_3 (\bar{N}_L \chi)_{1'} \nu_{R\tau} + \text{h.c.} \quad (2) \\
&= y_1 (\bar{\ell}_e N_{R_1} \tilde{\eta}_1 + \bar{\ell}_e N_{R_2} \tilde{\eta}_2 + \bar{\ell}_e N_{R_3} \tilde{\eta}_3) + y_2 (\bar{\ell}_\mu N_{R_1} \tilde{\eta}_1 + \omega \bar{\ell}_\mu N_{R_2} \tilde{\eta}_2 + \omega^2 \bar{\ell}_\mu N_{R_3} \tilde{\eta}_3) \\
&\quad + y_3 (\bar{\ell}_\tau N_{R_1} \tilde{\eta}_1 + \omega^2 \bar{\ell}_\tau N_{R_2} \tilde{\eta}_2 + \omega \bar{\ell}_\tau N_{R_3} \tilde{\eta}_3) + M_N \bar{N}_{L_1} N_{R_1} + M_N \bar{N}_{L_2} N_{R_2} + M_N \bar{N}_{L_3} N_{R_3} \\
&\quad + y'_1 (\bar{N}_{L_1} \chi_1 + \bar{N}_{L_2} \chi_2 + \bar{N}_{L_3} \chi_3) \nu_{Re} + y'_2 (\bar{N}_{L_1} \chi_1 + \omega \bar{N}_{L_2} \chi_2 + \omega^2 \bar{N}_{L_3} \chi_3) \nu_{R\mu} \\
&\quad + y'_3 (\bar{N}_{L_1} \chi_1 + \omega^2 \bar{N}_{L_2} \chi_2 + \omega \bar{N}_{L_3} \chi_3) \nu_{R\tau} + \text{h.c.} \quad (3)
\end{aligned}$$

where the A_4 product rules, given in Appendix A, have been used to write the interactions in component form. The scalar potential of the model is given in Appendix B. The Yukawa Lagrangian for charged leptons given by Eq. (1) gives rise to a diagonal charged lepton mass matrix. At tree level the neutral fermion mass matrices in the (ν_L, N_R) , (N_L, ν_R) , (N_L, N_R)

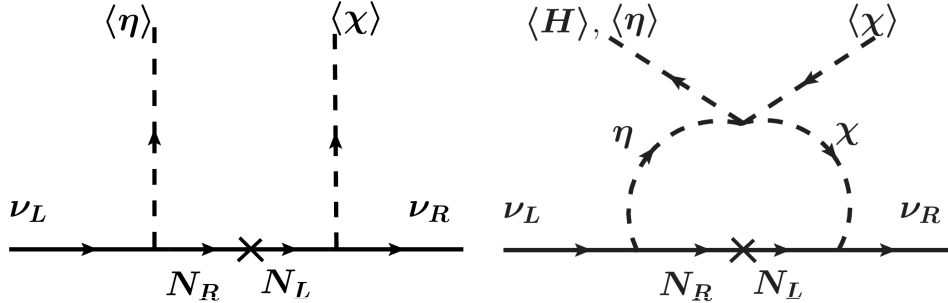


FIG. 1: Neutrino mass generation at tree level and one-loop level.

basis can be written as

$$m_D = v_\eta \begin{pmatrix} y_1 & 0 & 0 \\ y_2 & 0 & 0 \\ y_3 & 0 & 0 \end{pmatrix}, m'_D = v_\chi \begin{pmatrix} y'_1 & y'_2 & y'_3 \\ 0 & 0 & 0 \\ 0 & 0 & 0 \end{pmatrix}, M_R = \begin{pmatrix} M_N & 0 & 0 \\ 0 & M_N & 0 \\ 0 & 0 & M_N \end{pmatrix}; \quad (4)$$

where the vacuum expectation values (VEVs) of the A_4 scalar triplets are considered to be $\langle \eta \rangle = (\langle \eta_1 \rangle, \langle \eta_2 \rangle, \langle \eta_3 \rangle) = (\frac{v_\eta}{\sqrt{2}}, 0, 0)$ and $\langle \chi \rangle = (\langle \chi_1 \rangle, \langle \chi_2 \rangle, \langle \chi_3 \rangle) = (\frac{v_\chi}{\sqrt{2}}, 0, 0)$. Denoting the VEV of the neutral component of the Higgs doublet H as v , we have the constraint $\sqrt{v_\eta^2 + v^2} = 246$ GeV from the requirement of desired electroweak symmetry breaking (EWSB). Therefore, at three level, via type-I seesaw like scenario (shown in the left panel of Fig. 1), the light Dirac neutrino mass matrix can be written as

$$m_{\nu 0} = -m_D M_R^{-1} m'_D = -\frac{v_\eta v_\chi}{2M_N} \begin{pmatrix} y_1 y'_1 & y_1 y'_2 & y_1 y'_3 \\ y_2 y'_1 & y_2 y'_2 & y_2 y'_3 \\ y_3 y'_1 & y_3 y'_2 & y_3 y'_3 \end{pmatrix}. \quad (5)$$

Clearly, the tree level neutrino mass matrix is a matrix of rank-1 predicting only one massive neutrino with mass $m_0 = -\frac{v_\eta v_\chi}{2M_N} (y_1 y'_1 + y_2 y'_2 + y_3 y'_3)$.

At one-loop, all the A_4 triplet scalars $\eta = (\eta_1, \eta_2, \eta_3)$ and $\chi = (\chi_1, \chi_2, \chi_3)$ irrespective of their VEVs can contribute to light neutrino mass, as shown in the right panel of Fig. 1. This contribution is similar to the Dirac scotogenic model discussed in several earlier works [23, 29, 31, 34, 36, 50, 51, 85–92]. The one-loop contribution to light Dirac neutrino mass can be estimated as

$$m_{\nu}^{\text{loop}} = \sum_{j=1}^3 Y_{kj} Y'_{jl} M_j \mathcal{F}_j, \quad (6)$$

where

$$\mathcal{F}_j = \sum_{k,l} \frac{\sin \theta_{kl} \cos \theta_{kl}}{32\pi^2} \left(\frac{m_{\xi_k}^2}{m_{\xi_k}^2 - M_j^2} \ln \frac{m_{\xi_k}^2}{M_j^2} - \frac{m_{\xi_l}^2}{m_{\xi_l}^2 - M_j^2} \ln \frac{m_{\xi_l}^2}{M_j^2} \right), \quad (7)$$

with m_{ξ_k}, m_{ξ_l} being the mass eigenstates of the associated scalars, θ_{kl} being the mixing angle and $M_j = M_N$. Following Eq. (3), the Yukawa matrices Y, Y' involved in the scotogenic contribution above can be written as

$$Y = \begin{pmatrix} y_1 & y_1 & y_1 \\ y_2 & \omega y_2 & \omega^2 y_2 \\ y_3 & \omega^2 y_3 & \omega y_3 \end{pmatrix}, \quad Y' = \begin{pmatrix} y'_1 & y'_2 & y'_3 \\ y'_1 & \omega y'_2 & \omega^2 y'_3 \\ y'_1 & \omega^2 y'_2 & \omega y'_3 \end{pmatrix}. \quad (8)$$

Using these, the complete one-loop mass matrix for light Dirac neutrinos can be written as

$$\begin{aligned}
m_\nu^{\text{loop}} &= Y_{k1} Y'_{1l} M_N \mathcal{F}_1 + Y_{k2} Y'_{2l} M_N \mathcal{F}_2 + Y_{k3} Y'_{3l} M_N \mathcal{F}_3 \tag{9} \\
&= M_N \begin{pmatrix} y_1 y'_1 (\mathcal{F}_1 + \mathcal{F}_2 + \mathcal{F}_3) & y_1 y'_2 (\mathcal{F}_1 + \omega \mathcal{F}_2 + \omega^2 \mathcal{F}_3) & y_1 y'_3 (\mathcal{F}_1 + \omega^2 \mathcal{F}_2 + \omega \mathcal{F}_3) \\ y_2 y'_1 (\mathcal{F}_1 + \omega \mathcal{F}_2 + \omega^2 \mathcal{F}_3) & y_2 y'_2 (\mathcal{F}_1 + \omega^2 \mathcal{F}_2 + \omega \mathcal{F}_3) & y_2 y'_3 (\mathcal{F}_1 + \mathcal{F}_2 + \mathcal{F}_3) \\ y_3 y'_1 (\mathcal{F}_1 + \omega^2 \mathcal{F}_2 + \omega \mathcal{F}_3) & y_3 y'_2 (\mathcal{F}_1 + \mathcal{F}_2 + \mathcal{F}_3) & y_3 y'_3 (\mathcal{F}_1 + \omega \mathcal{F}_2 + \omega^2 \mathcal{F}_3) \end{pmatrix} \tag{10}
\end{aligned}$$

Therefore, the light Dirac neutrino mass matrix, taking tree level and one-loop contributions, can be written as

$$m_\nu = m_{\nu 0} + m_\nu^{\text{loop}} = \begin{pmatrix} (m_\nu)_{11} & (m_\nu)_{12} & (m_\nu)_{13} \\ (m_\nu)_{21} & (m_\nu)_{22} & (m_\nu)_{23} \\ (m_\nu)_{31} & (m_\nu)_{32} & (m_\nu)_{33} \end{pmatrix} \tag{11}$$

with the details of the components $(m_\nu)_{ij}$ being given in Appendix C. This mass matrix has rank 3 and predict three non-zero mass eigenvalues, in general. Also, it does not possess any specific symmetric structure and hence can be fitted to neutrino mixing data by appropriate choice of parameters, as we discuss below.

It should be noted that the above choice of VEV alignment leaves a remnant $\mathcal{Z}_2 \subset A_4$ unbroken after spontaneous symmetry breaking. The following fields transform non-trivially under this remnant symmetry as

$$\mathcal{Z}_2 : \eta_{2,3} \rightarrow -\eta_{2,3}; \quad \chi_{2,3} \rightarrow -\chi_{2,3}; \quad N_{2,3} \rightarrow -N_{2,3} \tag{12}$$

while all other fields are \mathcal{Z}_2 -even. The lightest \mathcal{Z}_2 -odd particle, therefore, is stable and can be a dark matter candidate, the details of which are discussed in section IV.

III. FIT TO NEUTRINO DATA

The effective Dirac neutrino mass matrix obtained in our framework is constituted by both tree level type-I Dirac seesaw contribution as well as one-loop Dirac scotogenic contributions as shown in Fig. 1. The effective neutrino mass matrix, given in Eq. (11), is dependent on the associated Yukawa couplings, scalar and fermion mass parameters, and mixing of the scalar mass eigenstates. Owing to the considered discrete flavour symmetry, here, both

Dirac type-I seesaw and scotogenic contributions share the same Yukawa couplings. Hence, as a consequence, the Yukawa couplings y_i, y'_i both appear in these two contributions, given in Eq. (5) and (10) respectively. Furthermore, same pair of these Yukawa couplings emerges in both Dirac type-I seesaw and scotogenic contributions in each element of the effective neutrino mass matrix, see Appendix C for details. The procured light neutrino mass matrix m_ν takes the most general form, having the ability to reproduce correct neutrino mixing corresponding to a wide range of the associated parameters. Therefore to explain the observed neutrino oscillation data [93, 94], for simplicity, we consider three benchmark cases for the Yukawa couplings y_i, y'_i such as: Case-A when $y_i \gg y'_i$, Case-B when $y_i \ll y'_i$ and Case-C when $y_i \simeq y'_i$ respectively. Based on these classifications of the Yukawa couplings, to reproduce correct light neutrino mass, we restrict the flavon VEVs to be around or above the electroweak scale while the M_N is found to lie in multi-TeV range from the fitting. In each of these cases, we consider the 3σ allowed range of neutrino oscillation data [93] on the mixing angles $\theta_{12}, \theta_{23}, \theta_{13}$, mass-squared differences $\Delta m_{21}^2, \Delta m_{31}^2$ and their ratio $\Delta m_{21}^2/\Delta m_{31}^2$ to obtain the constraints on the parameters appearing in the light Dirac neutrino mass matrix. In the subsequent sections we will explore the viability of these three benchmark scenarios to obtain dark matter relic density, direct search constraints and ΔN_{eff} elucidating a flavour symmetric origin for these observables. For brevity here we explicitly show the analysis for the normal hierarchy, however such an analysis can also be obtained for inverted hierarchy of the neutrino masses.

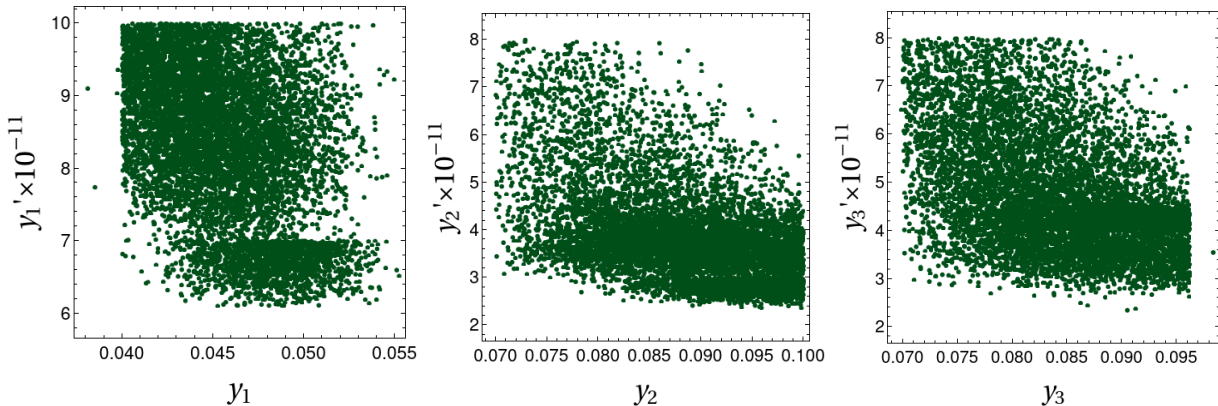


FIG. 2: Allowed regions for y_i, y'_i for the 3σ ranges for neutrino oscillation data for $y_i \gg y'_i$ (Case-A).

Case-A: We first consider the limiting case $y_i \gg y'_i$ for the associated Yukawa couplings. Corresponding to the 3σ range of neutrino oscillation data [93], the allowed ranges for y_i, y'_i

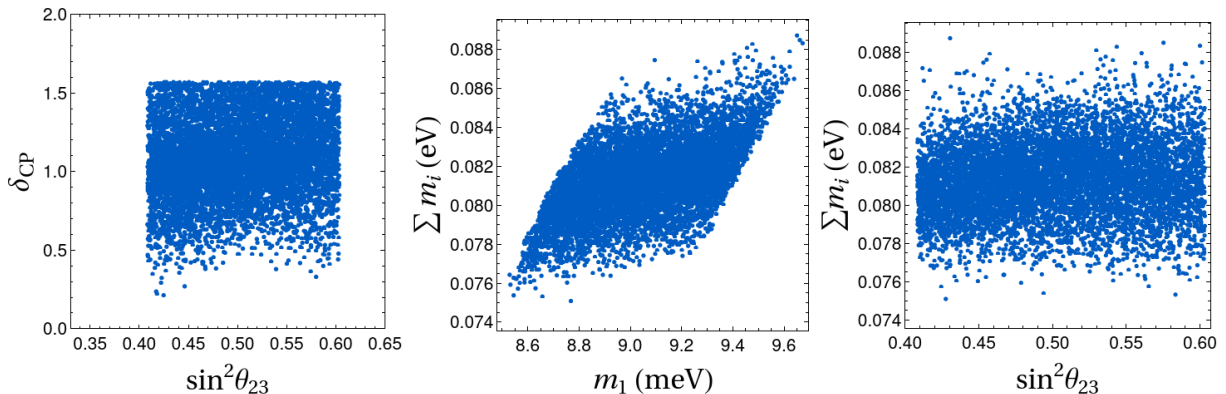


FIG. 3: Correlation for $\delta_{CP} - \sin^2 \theta_{23}$, $\sum m_i - m_1$, $\sum m_i - \sin^2 \theta_{23}$ for $y_i \gg y'_i$ (Case-A).

are given in $y'_1 - y_1$, $y'_2 - y_2$ and $y'_3 - y_3$ planes respectively, plotted in Fig. 2. In this benchmark scenario, y'_i are found to be in the range $0.6 \times 10^{-11} \leq y'_1 \leq 10^{-10}$, $2.3 \times 10^{-11} \leq y'_2 \leq 8 \times 10^{-11}$, $2.35 \times 10^{-11} \leq y'_3 \leq 8 \times 10^{-11}$ and corresponding ranges for y_i are found to be $0.038 \leq y_1 \leq 0.055$, $0.07 \leq y_2 \leq 0.1$ and $0.07 \leq y_3 \leq 0.098$ respectively. To be in agreement with neutrino oscillation data, other parameters are restricted within the range $3 \text{ TeV} \leq M_N \leq 5 \text{ TeV}$, $130 \leq (v_\eta/\text{GeV}) \leq 240$, $180 \leq (v_\chi/\text{GeV}) \leq 250$ with the loop functions defined in Eq. (7) having the magnitude $\mathcal{F}_i \sim \mathcal{O}(10^{-4})$. With the estimation of the parameters appearing in the neutrino mass matrix, we are now in a position to show the correlation among neutrino oscillation parameters as shown in Fig. 3. In this figure, we have plotted the correlations for $\delta_{CP} - \sin^2 \theta_{23}$, $\sum m_i - m_1$, $\sum m_i - \sin^2 \theta_{23}$ planes for Case-A and predicted ranges for δ_{CP} , $\sum m_i$ and m_1 are found to be in the range (0.2 – 1.6) radian, (0.075 – 0.089) eV and (8.5 – 9.7) meV respectively.

Case-B: We now consider the benchmark scenario, $y_i \ll y'_i$. Using similar methodology, we can again constrain the Yukawa couplings y_i, y'_i imposing the constraints on neutrino masses and mixing angles [93]. In Fig. 4 we have plotted the allowed values of the respective Yukawa couplings in $y'_1 - y_1$, $y'_2 - y_2$ and $y'_3 - y_3$ planes and y_i, y'_i are found to be restricted within the range $1.4 \times 10^{-11} \leq y_1 \leq 2.5 \times 10^{-11}$, $2 \times 10^{-11} \leq y_2 \leq 7 \times 10^{-11}$, $3.4 \times 10^{-11} \leq y_3 \leq 5.57 \times 10^{-11}$ and $0.01 \leq y'_1 \leq 0.1$, $0.03 \leq y'_2 \leq 0.1$, $0.04 \leq y'_3 \leq 0.1$ respectively. In order to satisfy the neutrino oscillation data, other parameters are restricted within the range

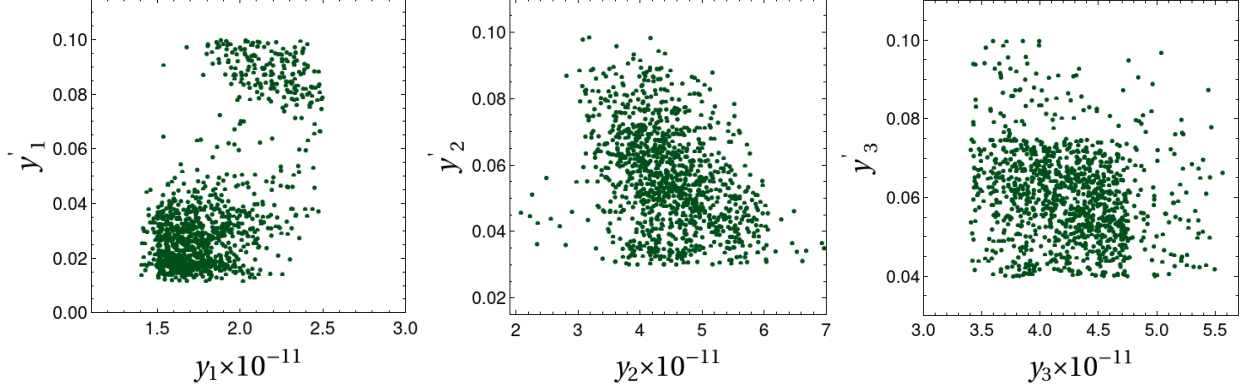


FIG. 4: Allowed regions for y_i, y'_i for the 3σ ranges for neutrino oscillation data for $y_i \ll y'_i$ (Case-B).

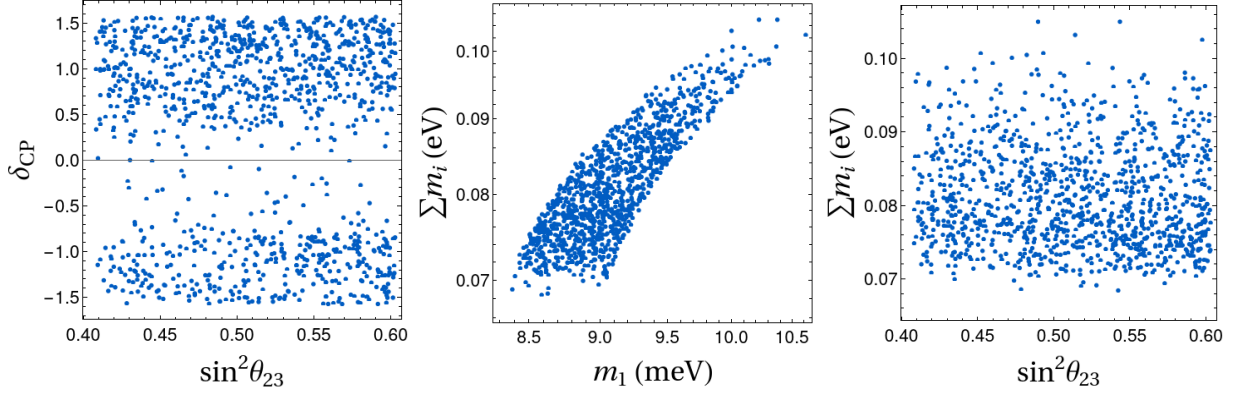


FIG. 5: Correlation for $\delta_{CP} - \sin^2 \theta_{23}$, $\sum m_i - m_1$ and $\sum m_i - \sin^2 \theta_{23}$ for $y_i \ll y'_i$ (Case-B).

$6 \text{ TeV} \leq M_N \leq 10 \text{ TeV}$, $120 \leq (v_\eta/\text{GeV}) \leq 240$, $100 \leq (v_\chi/\text{GeV}) \leq 700$. Corresponding loop functions \mathcal{F}_i , defined in Eq. (7), appearing in the Dirac scotogenic contribution are found to be in the range $5 \times 10^{-4} \leq \mathcal{F}_1 \leq 7 \times 10^{-4}$, $3 \times 10^{-4} \leq \mathcal{F}_2 \leq 10^{-3}$, $8 \times 10^{-4} \leq \mathcal{F}_3 \leq 1.3 \times 10^{-3}$. After estimating the parameters relevant for light neutrino mass matrix, we proceed to find some correlations among neutrino oscillation parameters as shown in Fig. 5. In this figure, we have plotted the correlations for $\delta_{CP} - \sin^2 \theta_{23}$, $\sum m_i - m_1$, $\sum m_i - \sin^2 \theta_{23}$ planes for the scenario $y_i \ll y'_i$ and predicted ranges for δ_{CP} , $\sum m_i$ and m_1 are found to be in the range $\pm(0 - 1.5)$ radian, $(0.068 - 0.11)$ eV and $(8.4 - 10.5)$ meV respectively.

Case-C Finally, we now consider the third benchmark scenario where $y_i \simeq y'_i$. In this scenario, one can also satisfy the observed constraints on neutrino masses and mixing where

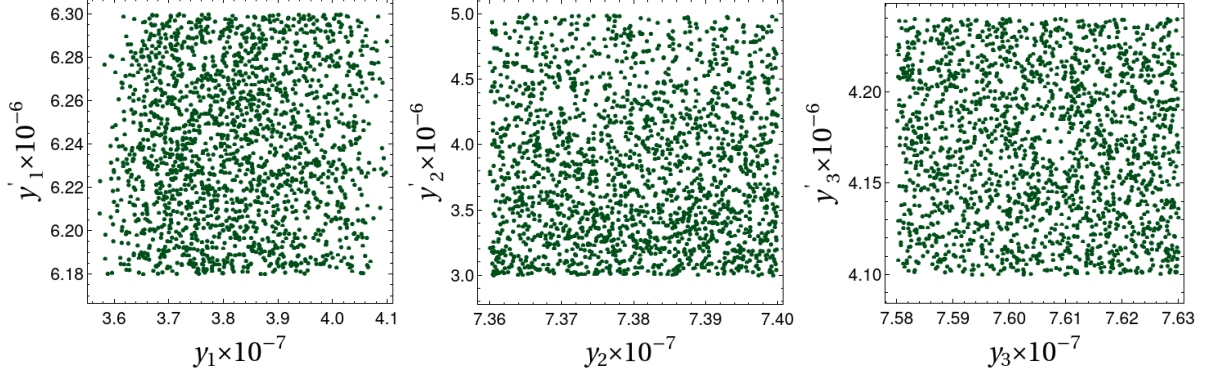


FIG. 6: Allowed regions for y_i, y'_i for the 3σ ranges for neutrino oscillation data for $y_i \simeq y'_i$ (Case-C).

the associated Yukawa couplings are found to be in the range $3.56 \times 10^{-7} \leq y_1 \leq 4.1 \times 10^{-7}$, $7.36 \times 10^{-7} \leq y_2 \leq 7.4 \times 10^{-7}$, $7.58 \times 10^{-7} \leq y_3 \leq 7.63 \times 10^{-7}$ and $6.18 \times 10^{-6} \leq y'_1 \leq 6.3 \times 10^{-6}$, $3 \times 10^{-6} \leq y'_2 \leq 5 \times 10^{-6}$ and $4.1 \times 10^{-6} \leq y'_3 \leq 4.25 \times 10^{-6}$ respectively. These allowed ranges are plotted in $y'_i - y_i$ planes as given in Fig. 6. To fit the model with the

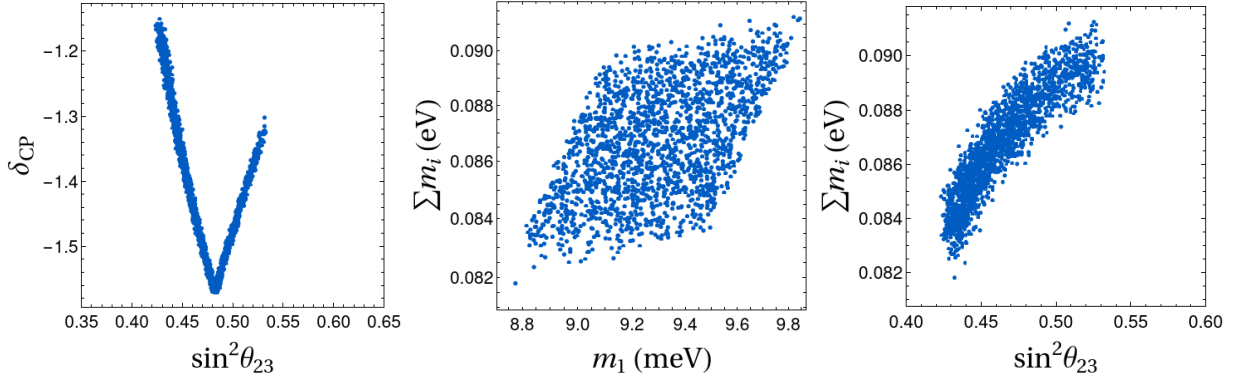


FIG. 7: Correlation for $\delta_{CP} - \sin^2 \theta_{23}$, $\sum m_i - m_1$ and $\sum m_i - \sin^2 \theta_{23}$ for $y_i \simeq y'_i$ (Case-C).

neutrino oscillation data in this scenario, other parameters are restricted within the range $11.4 \text{ TeV} \leq M_N \leq 14 \text{ TeV}$, $170 \leq (v_\eta/\text{GeV}) \leq 240$, $1 \leq (v_\chi/\text{TeV}) \leq 1.4$. Similarly, loop functions \mathcal{F}_i defined in Eq. (7), appearing in the Dirac scotogenic contribution are found to be in the range $10^{-3} \leq \mathcal{F}_1 \leq 1.2 \times 10^{-3}$, $4 \times 10^{-4} \leq \mathcal{F}_2 \leq 5 \times 10^{-4}$, $10^{-4} \leq \mathcal{F}_3 \leq 1.7 \times 10^{-4}$. Similar to the other two cases, here also we show the correlation among neutrino oscillation parameters in Fig. 7. In this figure, we have plotted the correlations for $\delta_{CP} - \sin^2 \theta_{23}$, $\sum m_i - m_1$, $\sum m_i - \sin^2 \theta_{23}$ planes for the current scenario and predicted ranges for δ_{CP} , $\sum m_i$ and m_1 are found to be in the range $-(1.57 - 1.5)$ radian, $(0.082 - 0.091)$ eV and

(8.8 – 9.8) meV respectively.

In the following sections, for compactness, we will consider these three benchmark scenarios for studies on scalar/fermionic WIMP dark matter, ΔN_{eff} and LFV decays associated with this discrete dark matter model for Dirac neutrinos.

IV. DARK MATTER

In this model, gauge singlet Dirac fermions $N_{2,3}$, gauge singlet scalars $\chi_{2,3}$ and $SU(2)$ doublet scalars $\eta_{2,3}$, remain odd under the residual \mathcal{Z}_2 symmetry such that the lightest among them becomes a viable dark matter candidate. When considering the fermionic dark matter scenario, *i.e.*, $M_N < M_\eta < M_\chi$, achieving the correct relic density becomes challenging because the mass M_N is constrained to the multi-TeV range by the neutrino mass criteria. Fermion DM in scotogenic model was studied in several earlier works, see [95–97] for example. As can be seen from these earlier works, fermion singlet DM relic relies primarily on Yukawa portal annihilations and coannihilations. Due to the involvement of the same Yukawa couplings in both type-I and scotogenic contributions to neutrino mass, we can not have Yukawa coupling in $\geq \mathcal{O}(1)$ regime as discussed in the previous section. After including coannihilation among fermion DM N and \mathcal{Z}_2 -odd scalars, correct relic abundance is found only for Case-A with $M_N \in [3000, 5000]$ GeV, considering the parameter space in agreement with neutrino data. However, for Case-B ($M_N \in [6000, 10000]$ GeV) and Case-C ($M_N \in [11400, 14000]$ GeV), where M_N is pushed to even larger values, it is not possible to achieve the correct relic density for the fermionic dark matter via thermal freeze-out. This is because the large M_N value and insufficient (co)annihilation rates always lead to an overabundant relic density. Thermal relic of N in Case-A is obtained due to smaller M_N and large coannihilation rate with $SU(2)$ doublet scalars via large Yukawa portal ($y_i \gg y'_i$) interactions. Since doublet scalars have more efficient annihilation rates, it is easier to obtain correct relic of N in Case-A compared to Case-B where N has sizeable Yukawa with scalars which are predominantly singlets. While Case-C offers the possibility of non-thermal or freeze-in fermion singlet DM, we find it to be overproduced as well leaving only Case-A as viable for fermion DM scenario.

In the case of scalar DM, the correct relic density can be obtained in all the three cases discussed in the previous section due to the gauge and scalar portal annihilation and co-

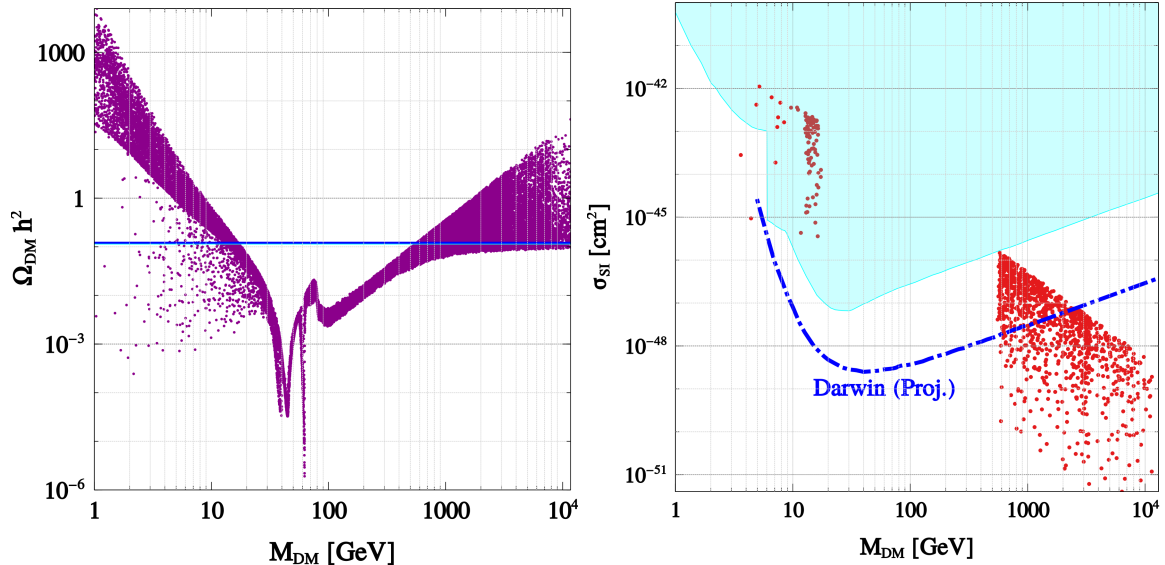


FIG. 8: Left panel: variation of scalar DM relic abundance with its mass. The blue solid line indicates the observed DM relic. Right panel: spin-independent DM-nucleon scattering as a function of the DM mass. The red colored points satisfy DM relic. The cyan shaded region is ruled out by direct detection constraints.

annihilation of the scalar DM while successfully explaining the neutrino data. Due to the possibility of additional portals namely gauge and scalar portals for annihilation, scalar DM relic can be obtained without relying on the Yukawa portal, unlike fermion singlet DM. With M_N varied in the required range so as to satisfy the neutrino oscillation data, we vary the masses of \mathcal{Z}_2 -odd scalars ζ_i (see Appendix B for the details of physical scalar masses and eigenstates) assuming two hierarchies $M_{\zeta_i} < M_N$ or $M_{\zeta_1} < M_N < M_{\zeta_j}, (j \neq 1)$. We consider ζ_1 , the lightest \mathcal{Z}_2 -odd scalar to be the DM. As the mass difference between ζ_i 's are constrained in a specific range from the neutrino mass criteria, when the mass hierarchy is $M_{\zeta_i} < M_N$, it is possible to get DM masses in the sub-TeV range. However when we assume the hierarchy $M_{\zeta_1} < M_N < M_{\zeta_j}, (j \neq 1)$, the DM mass always lies in the multi-TeV scale.

In the left panel of Fig. 8, we show the variation of scalar DM relic with its mass. As shown in several earlier works on scalar DM, the (co)annihilations mediated by electroweak gauge bosons and the SM Higgs are responsible for the dip for intermediate mass, leaving two distinct mass ranges satisfying correct relic. The right panel of the same figure shows the spin-independent DM-nucleon scattering cross-section (mediated via Higgs portal) as a function of scalar DM mass for the points which satisfy relic abundance criteria. We

used the package `MicrOMEGAs` [98] to calculate the relic density and DM-nucleon scattering cross-section after generating the model files using `LanHEP` [99]. The cyan shaded region is ruled out by the most stringent direct search constraints from LZ-2022 [60] for heavier DM and CRESST-III [100] and DarkSide-50 [101] for lighter DM. Clearly we can see that the viable DM mass range that satisfies correct relic density and direct detection rate ranges from around 500 GeV to several TeV scale. Interestingly, future direct detection experiment Darwin [102] can probe a part of this high mass region upto $M_{\text{DM}} \sim 3$ TeV.

V. OBSERVABLE ΔN_{eff}

The effective number of relativistic degrees of freedom N_{eff} defined as

$$N_{\text{eff}} = \frac{8}{7} \left(\frac{11}{4} \right)^{4/3} \left(\frac{\rho_R - \rho_\gamma}{\rho_\gamma} \right), \quad (13)$$

where ρ_R, ρ_γ denote total radiation and photon densities respectively. Existing data from CMB experiments like PLANCK constrains such additional light species by putting limits on the effective degrees of freedom for neutrinos during the era of recombination ($z \sim 1100$) as [59]

$$N_{\text{eff}} = 2.99^{+0.34}_{-0.33} \quad (14)$$

at 2σ or 95% C.L. including baryon acoustic oscillation (BAO) data. At 1σ C.L. it becomes more stringent to $N_{\text{eff}} = 2.99 \pm 0.17$. Similar bound also exists from big bang nucleosynthesis (BBN), $2.3 < N_{\text{eff}} < 3.4$ at 95% C.L. [103]. Recent observations by the DESI collaboration report $\Delta N_{\text{eff}} < 0.4$ [104], which is weaker than the PLANCK bound given in Eq. (14). All these bounds are consistent with SM predictions $N_{\text{eff}}^{\text{SM}} = 3.045$ [105–107]. Future CMB experiment CMB-S4 is expected reach a much better sensitivity of $\Delta N_{\text{eff}} = N_{\text{eff}} - N_{\text{eff}}^{\text{SM}} = 0.06$ [81], taking it closer to the SM prediction. Another future CMB experiment, specially, CMB-HD [84] can probe ΔN_{eff} upto 0.014 at 1σ . Dirac nature of light neutrinos introduces additional relativistic degrees of freedom in the form of right chiral neutrinos which can contribute to ΔN_{eff} either thermally or non-thermally. Light Dirac neutrino models often lead to enhanced ΔN_{eff} , some recent works on which can be found in [49, 52, 108–119]. Depending upon the strength of Yukawa couplings associated with ν_R , we can have either thermal or non-thermal contribution to ΔN_{eff} as we discuss in the following subsections.

A. Thermal ΔN_{eff}

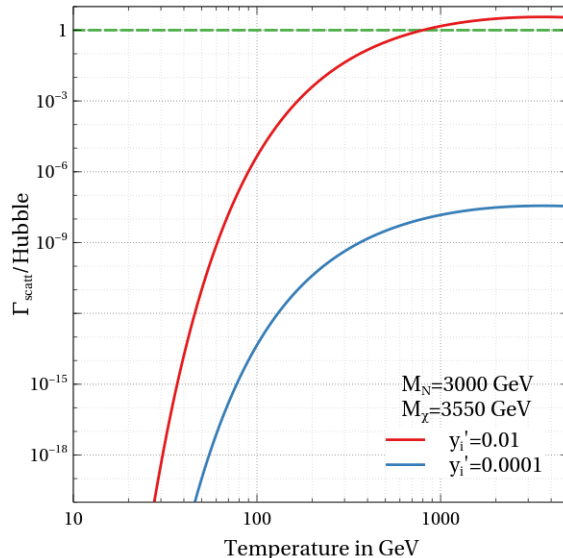


FIG. 9: Interaction rate of ν_R compared to the Hubble expansion rate, indicating its decoupling profile for two sets of benchmark values.

We have three generations of right handed neutrinos (ν_{R_i}) in our model, and their abundance in the Universe will be decided by the interaction strength and the masses of the particle with which they interact. The last three interaction terms of the Lagrangian (Eq. (2)) are the only three interactions that ν_R have with N and χ . The relative strength between the two types of Yukawa couplings y_i and y'_i leads to three distinctive classes (Case-A, Case-B, Case-C) as we discussed before, in the context of neutrino mass and DM. With sufficiently large Yukawa coupling (y'_i) as in Case-B, ν_R may enter the thermal bath with the SM degrees of freedom. As the Universe expands and the temperature falls, the scattering processes that kept ν_R in the thermal bath eventually go out of equilibrium, leading to the decoupling of ν_R . For the combined scattering processes of $N_L \bar{\nu}_R \leftrightarrow N_L \bar{\nu}_R$ and $\chi \bar{\nu}_R \leftrightarrow \chi \bar{\nu}_R$, we check the decoupling or thermalization profile with two sets of benchmark parameters (masses and couplings) as shown in Fig. 9. As N and χ masses lies at $\mathcal{O}(\text{TeV})$ range, it leads to the decoupling of ν_R from the thermal bath very early. Such early decoupling, above the electroweak scale, leads to a fixed value $\Delta N_{\text{eff}} = 0.14$ for three generations of ν_R . Clearly, this remains within reach of several future CMB experiments mentioned earlier.

B. Non-thermal ΔN_{eff}

It is also possible to have observable ΔN_{eff} when ν_R does not enter the thermal bath. In such a case, ν_R can be produced non-thermally from the decay of the scalar χ as $\chi \rightarrow N\nu_{R_i}$ or from decay of N as $N \rightarrow \chi\nu_{R_i}$ depending upon our choice of fermion or scalar DM. Similar contributions can also arise from scatterings. With small Yukawa couplings for the $\bar{N}_L\chi\nu_R$ interaction (as in Case-A and Case-C), ν_R can not enter the thermal bath via the $N_L\bar{\nu}_R \leftrightarrow N_L\nu_R$ (or $\chi\bar{\nu}_R \leftrightarrow \chi\nu_R$) scattering process. In such a situation, where the scalar χ is in the thermal bath, ν_R are produced via the decay $\chi \rightarrow N\nu_R$ (assuming fermion DM scenario).

With χ in equilibrium and subsequently producing N and ν_R , the relevant Boltzmann equation for the comoving density of ν_R of flavour α is given by [120],

$$\frac{d\tilde{Y}_{\nu_R^\alpha}}{dx} = \frac{\beta}{x\mathcal{H}s^{1/3}} \langle E\Gamma \rangle Y_N^{\text{eq}}. \quad (15)$$

Here, $x = \frac{M_\chi}{T}$, \mathcal{H} is the Hubble parameter in the radiation dominated era and β is defined as $\beta = \left[1 + T \frac{dg_s/dT}{3g_s}\right]$ with g_s being the effective relativistic entropy degrees of freedom. For the sub-eV scale ν_R , which remains relativistic till recombination, the comoving energy density is defined as $\tilde{Y}_{\nu_R^\alpha} = \rho_{\nu_R^\alpha}/s^{4/3}$ with $\rho_{\nu_R^\alpha}, s$ denoting energy density of ν_R^α and entropy density of the Universe respectively. The quantity $\langle E\Gamma \rangle$ is defined as

$$\langle E\Gamma \rangle = g_N g_{\nu_R} \frac{|\mathcal{M}|_{\chi \rightarrow \bar{\nu}_R^\alpha N}^2 (M_\chi^2 - M_N^2)^2}{32\pi M_\chi^4}. \quad (16)$$

with g_i being the internal degrees of freedom of species "i" and $|\mathcal{M}|_{\chi \rightarrow \bar{\nu}_R^\alpha N}$ represents the decay amplitude. The ν_R produced from χ decay will contribute to this additional radiation density. Therefore, with $\rho_R = \rho_{\text{SM}} + \rho_{\nu_R}$, ΔN_{eff} for one species of ν_R (indicated by flavour index α) calculated at the CMB epoch (T_{CMB}) is

$$\begin{aligned} \Delta N_{\text{eff}}^\alpha &= N_{\text{eff}}^\alpha - N_{\text{eff}}^{\text{SM}} \\ &= 2 \times \left(\frac{\rho_{\nu_R^\alpha}}{\rho_{\nu_L}} \right)_{T_{\text{CMB}}} \\ &= 2 \times \left(\frac{\rho_{\nu_R^\alpha}}{\rho_{\nu_L}} \right)_{T_{\text{BBN}}} \\ &= 2 \times \left(\frac{s^{4/3} \tilde{Y}_{\nu_R^\alpha}}{\rho_{\nu_L}} \right)_{T_{\text{BBN}}} \end{aligned} \quad (17)$$

where, the extrapolation from the BBN epoch (T_{BBN}) to CMB epoch (T_{CMB}) is justified by the fact that both $\rho_{\nu_L}, \rho_{\nu_R}$ redshift similarly for $T < T_{\text{BBN}}$. One can simply calculate the

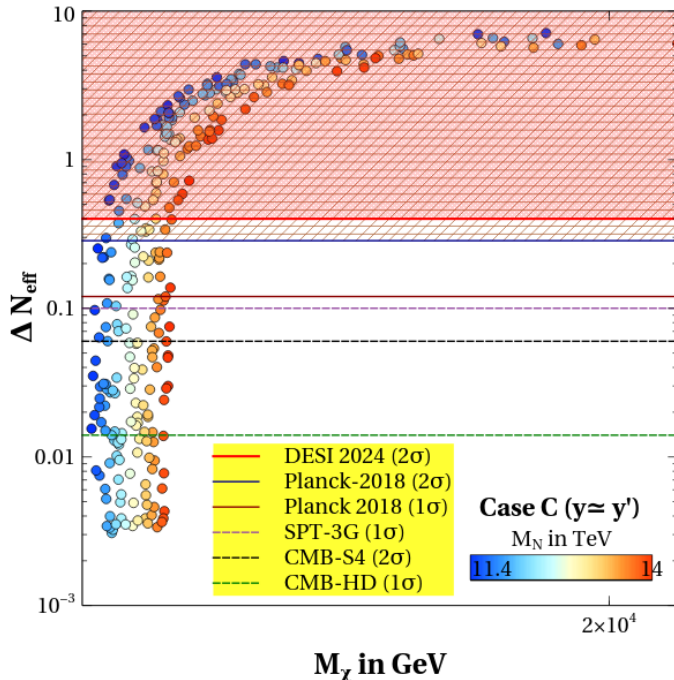


FIG. 10: Contribution to non-thermal ΔN_{eff} for the Case-C where $y'_i \sim \mathcal{O}(10^{-6})$, considering the decay $\chi \rightarrow \nu_R N$.

energy density ratio at BBN epoch $\sim \mathcal{O}(10)$ MeV as ν_R production stops much earlier. The numerical factor 2 in Eq. (17) indicate the degrees of freedom of each ν_R . The net contribution to ΔN_{eff} can be obtained by summing over flavour index α as $\Delta N_{\text{eff}} = \sum_{\alpha} \Delta N_{\text{eff}}^{\alpha}$.

The decoupling profile for ν_R for two different benchmark choices of Yukawa coupling y'_i is shown in Fig. 9. For scalar (χ) and fermion (N) masses in the TeV ballpark, we find that for $y'_i \leq \mathcal{O}(10^{-3})$, the interaction $N_L \bar{\nu}_R \leftrightarrow N_L \bar{\nu}_R$ can not attain thermal equilibrium in the early Universe. Therefore, Case-A with $y'_i \sim \mathcal{O}(10^{-11})$, ν_R will never enter the thermal bath, hence, thermal ΔN_{eff} is not possible. On the other hand, ν_R produced non-thermally from the decay of either χ or N gives rise to negligible contribution to ΔN_{eff} . As mentioned before, the Case-B, with $0.01 \leq y'_1 \leq 0.1$, $0.03 \leq y'_2 \leq 0.1$, $0.03 \leq y'_3 \leq 0.1$, we have thermal contribution to ΔN_{eff} . Due to decoupling of ν_R much above the electroweak scale, we have a fixed contribution $\Delta N_{\text{eff}} = 0.14$ for Case-B. Finally, in Case-C, Yukawa couplings are of the size $\mathcal{O}(10^{-6})$, and the corresponding interactions do not allow ν_R to enter the thermal bath. Considering the decay of $\chi \rightarrow \nu_R N$, we have shown the non-thermal contributions to ΔN_{eff} in Fig. 10. Clearly, some part of the parameter space is already ruled out by PLANCK

2018 and DESI 2024 limits while most of the remaining parameter space remains within reach of future CMB experiments like SPT-3G, CMB-S4 and CMB-HD. Similar results can be obtained by considering the decay mode $N \rightarrow \nu_R \chi$ applicable for scalar DM, without changing the conclusion significantly.

To summarise, observable ΔN_{eff} is possible in Case-B and Case-C. However, fermion DM is not possible in these two cases irrespective of freeze-out or freeze-in mechanism. On the other hand, fermion DM produced via freeze-out mechanism is viable in Case-A even though the ΔN_{eff} remains out of reach from future CMB experiments. This conflict between observable ΔN_{eff} and DM relic can be avoided if we consider scalar DM. Scalar DM allows light scalars in sub-TeV ballpark with observable direct detection rates while keeping collider prospects more promising compared to fermion DM scenario where all \mathcal{Z}_2 -odd particles remain in multi-TeV ballpark.

VI. OTHER DETECTION PROSPECTS

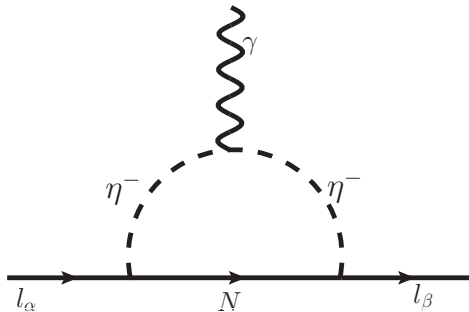


FIG. 11: One-loop contribution to charged lepton flavour violating $l_\eta \rightarrow l_\alpha \gamma$ process

In addition to the detection possibilities of DM and ΔN_{eff} , the model can have other detection aspects too. We briefly comment on such possibilities here.

Firstly, we can have a lepton flavour violating (LFV) process at one-loop level, as shown in Fig. 11. The corresponding decay width can be calculated using the prescriptions given in [50, 121]. With relevant Yukawa couplings of $y_i \sim \mathcal{O}(10^{-1} - 10^{-2})$, as in Case-A, it gives the branching ratio $\text{Br}(\mu \rightarrow e \gamma) \sim \mathcal{O}(10^{-15})$, which is close to the recent upper bound indicated by MEG-II experiment $\text{Br}(\mu \rightarrow e \gamma) < 3.1 \times 10^{-13}$ [122]. For Case-B and Case-C with smaller Yukawa couplings $y_i \sim \mathcal{O}(10^{-11})$ and $y_i \sim \mathcal{O}(10^{-7})$, we get very small branching

ratio $\text{Br}(\mu \rightarrow e\gamma)$ as $\mathcal{O}(10^{-57})$ and $\mathcal{O}(10^{-41})$ respectively, beyond experimental reach in near future.

Due to the presence of several new scalars, admixtures of singlet and doublet, we can have different collider prospects as well. If scalar DM mass (M_χ) is lighter than the SM Higgs mass (M_h) such that $h \rightarrow \chi\chi$ decay is allowed, it can contribute to invisible Higgs decay. Such invisible Higgs decay is currently constrained at $\text{Br}(h \rightarrow \text{invisible}) < 0.14$ [123]. Production of \mathcal{Z}_2 -odd scalars in colliders like the large hadron collider (LHC) can give rise to pure leptonic final states plus missing transverse energy (MET) [124, 125], hadronic final states plus MET [126] or a mixture of both. Such MET can arise from light Dirac neutrinos or scalar/fermion DM in our scenario. It is also possible to have more exotic signatures like tri-lepton plus MET [127] and mono-jet [128, 129]. It should be noted that we also have new scalars in the model which are \mathcal{Z}_2 -even. They can lead to additional final states, similar to generic two Higgs doublet models. The new charged scalars can also modify the diphoton decay width of the SM Higgs, currently constrained at $\frac{\text{BR}(h \rightarrow \gamma\gamma)_{\text{expt}}}{\text{BR}(h \rightarrow \gamma\gamma)_{\text{SM}}} = 1.12 \pm 0.09$ [130].

Another interesting detection prospect arises in the gravitational wave (GW) frontier. Spontaneous breaking of discrete symmetries like $A_4 \times \mathcal{Z}_2$, as we have in our model, can lead to formation of topological defects like domain walls (DW). While DW, if stable or allowed to dominate the energy density of the Universe, will be in conflict with cosmological observations, they can be made to disappear by introducing small bias, in the form of explicit symmetry breaking terms. Such annihilating or collapsing DW then generates stochastic GW which can be probed at ongoing or future experiments. GW signatures of minimal Dirac seesaw model was studied in earlier works [131, 132] while similar studies in the context of flavour symmetric models like A_4 can be found in [133]. The bias or explicit symmetry breaking terms introduced for DW disappearance may also lead to interesting indirect detection signatures of DM due to its decay into different standard model particles¹. While the model has several detection prospects, it can also be falsified by future observation of neutrinoless double beta decay.

¹ See [134, 135] for related discussions.

Case	Yukawa Coupling	Neutrino Data	Observable ΔN_{eff} (Thermal)	Observable ΔN_{eff} (Non-thermal)	Fermion DM	Scalar DM	Observable LFV
A	$y_i \gg y'_i$	Yes	No	No	Yes	Yes	Yes
B	$y_i \ll y'_i$	Yes	Yes	Not applicable	No	Yes	No
C	$y_i \simeq y'_i$	Yes	No	Yes	No	Yes	No

TABLE II: Summary of results for three benchmark scenarios.

VII. CONCLUSION

We have proposed a new model of light Dirac neutrinos based on non-Abelian discrete flavour symmetry A_4 augmented with $Z_2 \times U(1)_L$ where the symmetry breaking pattern leaves a remnant $\mathcal{Z}_2 \subset A_4$ symmetry responsible for stabilising DM. Using the minimal flavon and additional fermion content required for realising neutrino data, we take both tree level and one-loop contributions to light Dirac neutrino masses. The remnant \mathcal{Z}_2 symmetry allows either fermion or scalar DM candidates. While scalar DM is dominantly produced thermally due to gauge and scalar portal interactions, fermion DM production relies primarily on Yukawa portal interactions. The same Yukawa portal interactions can also lead to thermal or non-thermal production of right handed neutrinos, which contribute to the effective relativistic degrees of freedom ΔN_{eff} . To illustrate this, we consider three different benchmark scenarios of such Yukawa couplings and perform a detailed study of neutrino mass, mixing together with DM and ΔN_{eff} . We also check the scope of other detection prospects like LFV decays. Table II summarises our results. While one of the sub-classes of Yukawa couplings, namely Case-A, allows fermion singlet DM with observable LFV rates, the corresponding ΔN_{eff} remains negligible. The other two sub-classes allow scalar DM only but with observable ΔN_{eff} at future CMB experiments. The LFV rates however remain tiny in these two sub-classes. Due to the rich particle spectrum in terms of several scalar doublets and singlets, the model can also have rich collider phenomenology. On the other hand, spontaneous breaking of discrete symmetries can have interesting consequences in cosmology due to the formation of domain walls. Such walls, which disappear due to soft-breaking terms, can emit stochastic gravitational waves which can be probed at different ongoing and future experiments. The same soft-breaking terms can also lead to decay of DM, keeping indirect detection prospects alive. We leave a comprehensive analysis of such additional detection

prospects of our model to future works.

Acknowledgments

The work of D.B. is supported by the Science and Engineering Research Board (SERB), Government of India grants MTR/2022/000575 and CRG/2022/000603. The work of B.K. has been supported in part by the Polish National Science Center (NCN) under grant 2020/37/B/ST2/02371, the Freedom of Research, Mobility of Science, Research Excellence Initiative of the University of Silesia in Katowice and EU COST Action (CA21136). S.M. acknowledges the financial support from the National Research Foundation (NRF) grant funded by the Korea government (MEST) NRF-2022R1A2C1005050.

Appendix A: A_4 Multiplication Rules:

All finite groups are completely characterized by means of a set of elements called generators of the group and a set of relations, so that all the elements of the group are given as product of the generators. The group A_4 consists of the even permutations of four objects and then contains $4!/2 = 12$ elements. The generators are S and T with the relations $S^2 = T^3 = (ST)^3 = \mathcal{I}$, then the elements are $1, S, T, ST, TS, T^2, ST^2, STS, TST, T^2S, TST^2, T^2ST$.

It has four irreducible representations: three one-dimensional and one three-dimensional which are denoted by $\mathbf{1}, \mathbf{1}', \mathbf{1}''$ and $\mathbf{3}$ respectively. Under A_4 , one-dimensional unitary representations are given as,

$$\begin{aligned} \mathbf{1} \quad S &= 1 \quad T = 1 \\ \mathbf{1}' \quad S &= 1 \quad T = \omega \\ \mathbf{1}'' \quad S &= 1 \quad T = \omega^2 \end{aligned}$$

$\omega = e^{i\frac{2\pi}{3}}$ is cube root of unity. In the basis, where S is a real diagonal,

$$S = \begin{pmatrix} 1 & 0 & 0 \\ 0 & -1 & 0 \\ 0 & 0 & -1 \end{pmatrix} \quad T = \begin{pmatrix} 0 & 1 & 0 \\ 0 & 0 & 1 \\ 1 & 0 & 0 \end{pmatrix} \quad (\text{A1})$$

The multiplication rules of the irreducible representations are given by [63]

$$\mathbf{1} \otimes \mathbf{1} = \mathbf{1}, \mathbf{1}' \otimes \mathbf{1}' = \mathbf{1}'', \mathbf{1}' \otimes \mathbf{1}'' = \mathbf{1}, \mathbf{1}'' \otimes \mathbf{1}'' = \mathbf{1}', \mathbf{3} \otimes \mathbf{3} = \mathbf{1} + \mathbf{1}' + \mathbf{1}'' + \mathbf{3}_a + \mathbf{3}_s \quad (\text{A2})$$

where \mathbf{a} and \mathbf{s} in the subscript corresponds to anti-symmetric and symmetric parts respectively. Now, if we have two triplets as $A = (a_1, a_2, a_3)^T$ and $B = (b_1, b_2, b_3)^T$ respectively, their direct product can be decomposed into the direct sum mentioned above. The product rule for this two triplets in the S diagonal basis² can be written as [136]

$$(A \times B)_{\mathbf{1}} \sim a_1 b_1 + a_2 b_2 + a_3 b_3, \quad (\text{A3})$$

$$(A \times B)_{\mathbf{1}'} \sim a_1 b_1 + \omega^2 a_2 b_2 + \omega a_3 b_3, \quad (\text{A4})$$

$$(A \times B)_{\mathbf{1}''} \sim a_1 b_1 + \omega a_2 b_2 + \omega^2 a_3 b_3, \quad (\text{A5})$$

$$(A \times B)_{\mathbf{3}_s} \sim (a_2 b_3 + a_3 b_2, a_3 b_1 + a_1 b_3, a_1 b_2 + a_2 b_1), \quad (\text{A6})$$

$$(A \times B)_{\mathbf{3}_a} \sim (a_2 b_3 - a_3 b_2, a_3 b_1 - a_1 b_3, a_1 b_2 - a_2 b_1), \quad (\text{A7})$$

here $\omega (= e^{2i\pi/3})$ is the cube root of unity.

Appendix B: The scalar potential

The tree level scalar potential of our model can be written as

$$\begin{aligned} V(H, \eta, \chi) = & -\mu_h^2 (H^\dagger H) - \mu_\eta^2 (\eta^\dagger \eta)_1 - \mu_\chi^2 (\chi \chi)_1 + \lambda_H (H^\dagger H)^2 + \lambda_{\eta 1} (\eta^\dagger \eta)_1 (\eta^\dagger \eta)_1 + \lambda_{\eta 2} (\eta^\dagger \eta)_{1'} (\eta^\dagger \eta)_{1''} \\ & + \lambda_{\eta 4} \left[\sum_{i,j} (\eta^\dagger \eta)_{3_i} (\eta^\dagger \eta)_{3_j} + \text{h.c.} \right] + \lambda_{\eta H 1} (\eta^\dagger \eta)_1 (H^\dagger H) + \lambda_{\eta H 2} (\eta^\dagger \eta) (H^\dagger H) \\ & + [\lambda'_{\eta H 1} (\eta^\dagger H) (\eta^\dagger H) + \text{h.c.}] + [\lambda_{\eta H 3} (\eta^\dagger \eta)_{3_1} H^\dagger \eta + \text{h.c.}] + [\lambda_{\eta H 4} (\eta^\dagger \eta)_{3_2} H^\dagger \eta + \text{h.c.}] \\ & + \lambda_{\chi 1} (\chi \chi)_1 (\chi \chi)_1 + \lambda_{\chi 2} (\chi \chi)_{1'} (\chi \chi)_{1''} + \lambda_{\chi 3} \left[\sum_{i,j} (\chi \chi)_{3_i} (\chi \chi)_{3_j} \right] + \lambda_{\chi H 1} (\chi \chi)_1 (H^\dagger H) \\ & + \lambda_{\eta \chi 1} (\eta^\dagger \eta)_1 (\chi \chi)_1 + \lambda_{\eta \chi 2} (\eta^\dagger \eta)_{1'} (\chi \chi)_{1''} + \lambda_{\eta \chi 3} (\eta^\dagger \eta)_{1''} (\chi \chi)_{1'} + \lambda_{\eta \chi 4} \sum_{i,j} (\eta^\dagger \eta)_{3_i} (\chi \chi)_{3_j} \\ & + [\lambda_{\eta H \chi} (\chi \chi)_{3_1} (H^\dagger \eta) + \text{h.c.}] + [\lambda'_{\eta H \chi} (\chi \chi)_{3_2} (H^\dagger \eta) + \text{h.c.}] \end{aligned} \quad (\text{B1})$$

where, the product of two triplets contracted into one of the two triplet representations of A_4 is indicated by $[\dots]_{3_{1,2}}$, and the product of two triplets contracted into a singlet is represented by $[\dots]_{1,1',1''}$. Among the A_4 triplet scalars $\eta = (\eta_1, \eta_2, \eta_3)$ and $\chi = (\chi_1, \chi_2, \chi_3)$, only η_1 and

² Here S is a 3×3 diagonal generator of A_4 .

χ_1 are getting VEV v_η and v_χ respectively. The scalar fields can be expressed as

$$H = \begin{pmatrix} h^\pm \\ (v + h + iA)/\sqrt{2} \end{pmatrix}; \quad (\text{B2})$$

$$\eta_1 = \begin{pmatrix} \eta_1^\pm \\ (v_\eta + h_1 + iA_1)/\sqrt{2} \end{pmatrix}; \quad \eta_{2,3} = \begin{pmatrix} \eta_{2,3}^\pm \\ (h_{2,3} + iA_{2,3})/\sqrt{2} \end{pmatrix} \quad (\text{B3})$$

$$\chi_1 = (v_\chi + x_1)/\sqrt{2}; \quad \chi_{2,3} = x_{2,3}/\sqrt{2}. \quad (\text{B4})$$

The minimisation conditions for the scalars obtaining non-zero VEVs can be written as

$$\mu_H^2 = \lambda_H v^2 + (\lambda_{\eta H1} + \lambda_{\eta H2} + 2\lambda'_{\eta H1}) \frac{v_\eta^2}{2} + \lambda_{\chi H1} \frac{v_\chi^2}{2}, \quad (\text{B5})$$

$$\mu_\eta^2 = (\lambda_{\eta 1} + \lambda_{\eta 2}) v_\eta^2 + (\lambda_{\eta H1} + \lambda_{\eta H2} + 2\lambda'_{\eta H1}) \frac{v^2}{2} + (\lambda_{\eta \chi 1} + \lambda_{\eta \chi 2} + \lambda_{\eta \chi 3}) \frac{v_\chi^2}{2}, \quad (\text{B6})$$

$$\mu_\chi^2 = (\lambda_{\chi 1} + \lambda_{\chi 1}) v_\chi^2 + \lambda_{\chi H1} \frac{v^2}{2} + (\lambda_{\eta \chi 1} + \lambda_{\eta \chi 2} + \lambda_{\eta \chi 3}) \frac{v_\eta^2}{2}. \quad (\text{B7})$$

There are seven neutral scalars ($h, h_1, h_2, h_3, x_1, x_2, x_3$) out of which four are \mathcal{Z}_2 -odd while the remaining three are \mathcal{Z}_2 -even. Similarly, there is one physical pseudo-scalar out of the \mathcal{Z}_2 -even combination of (A, A_1) while (A_2, A_3) constitute \mathcal{Z}_2 -odd pseudoscalars. The \mathcal{Z}_2 -even scalar mass matrix squared in the (h, h_1, x_1) basis can be written as

$$M_{S^+}^2 = \begin{pmatrix} M_{hh}^2 & M_{hh_1}^2 & M_{hx_1}^2 \\ M_{hh_1}^2 & M_{h_1h_1}^2 & M_{h_1x_1}^2 \\ M_{hx_1}^2 & M_{h_1x_1}^2 & M_{x_1x_1}^2 \end{pmatrix} \quad (\text{B8})$$

where

$$M_{hh}^2 = 8\lambda_H v^2 + 2(\lambda_{\eta H1} + \lambda_{\eta H2} + 2\lambda'_{\eta H1}) v_\eta^2 + 2\lambda_{\chi H1} v_\chi^2,$$

$$M_{hh_1}^2 = (\lambda_{\eta H1} + \lambda_{\eta H2} + 2\lambda'_{\eta H1}) v_\eta v, \quad M_{hx_1}^2 = \lambda_{\chi H1} v_\chi v,$$

$$M_{h_1h_1}^2 = 8(\lambda_{\eta 1} + \lambda_{\eta 2}) v_\eta^2 + 2(\lambda_{\eta H1} + \lambda_{\eta H2} + 2\lambda'_{\eta H1}) v^2 + 2(\lambda_{\eta \chi 1} + \lambda_{\eta \chi 2} + \lambda_{\eta \chi 3}) v_\chi^2,$$

$$M_{h_1x_1}^2 = (\lambda_{\eta \chi 1} + \lambda_{\eta \chi 2} + \lambda_{\eta \chi 3}) v_\chi v_\eta, \quad M_{x_1x_1}^2 = 8(\lambda_{\chi 1} + \lambda_{\chi 2}) v_\chi^2 + 2\lambda_{\chi H1} v^2 + 2(\lambda_{\eta \chi 1} + \lambda_{\eta \chi 2} + \lambda_{\eta \chi 3}) v_\eta^2.$$

This mass squared matrix can be diagonalised by 3×3 orthogonal matrix involving three angles. Similarly, the \mathcal{Z}_2 -odd scalar mass matrix squared in the (h_2, h_3, x_2, x_3) basis can be written as

$$M_{S^-}^2 = \begin{pmatrix} M_{h_2h_2}^2 & M_{h_2h_3}^2 & M_{h_2x_2}^2 & M_{h_2x_3}^2 \\ M_{h_2h_3}^2 & M_{h_3h_3}^2 & M_{h_3x_2}^2 & M_{h_3x_3}^2 \\ M_{h_2x_2}^2 & M_{h_3x_2}^2 & M_{x_2x_2}^2 & M_{x_2x_3}^2 \\ M_{h_2x_3}^2 & M_{h_3x_3}^2 & M_{x_2x_3}^2 & M_{x_3x_3}^2 \end{pmatrix}, \quad (\text{B9})$$

where

$$M_{h_2 h_2}^2 = 2(\lambda_{\eta 1} + \lambda_{\eta 2} + 2\lambda_{\eta 4})v_\eta^2 + (\lambda_{\eta H 1} + \lambda_{\eta H 2} + 2\lambda'_{\eta H 1})v^2 + (\lambda_{\eta \chi 1} + \lambda_{\eta \chi 2} + \lambda_{\eta \chi 3})v_\eta^2,$$

$$M_{h_2 h_3}^2 = \frac{3}{2}\lambda_{\eta H 3}vv_\eta, \quad M_{h_2 x_2}^2 = \lambda_{\eta \chi 4}v_\eta v_\chi$$

and so on. This mass squared matrix can similarly be diagonalised by a 4×4 orthogonal matrix involving six angles, in general, leading to physical states ζ_i . In the scalar DM case, the lightest eigenstate of the 4×4 mass matrix given above becomes the DM candidate. Similar mass matrices can be written for both \mathcal{Z}_2 -odd and \mathcal{Z}_2 -even pseudoscalars as well.

Appendix C: Neutrino mass matrix

$$m_\nu = m_{\nu 0} + m_\nu^{\text{loop}} \quad (\text{C1})$$

$$= \begin{pmatrix} (m_\nu)_{11} & (m_\nu)_{12} & (m_\nu)_{13} \\ (m_\nu)_{21} & (m_\nu)_{22} & (m_\nu)_{23} \\ (m_\nu)_{31} & (m_\nu)_{32} & (m_\nu)_{33} \end{pmatrix} \quad (\text{C2})$$

where,

$$(m_\nu)_{11} = -\frac{v_\eta v_\chi}{2M_N} y_1 y'_1 + y_1 y'_1 M_N (\mathcal{F}_1 + \mathcal{F}_2 + \mathcal{F}_3) \quad (\text{C3})$$

$$(m_\nu)_{12} = -\frac{v_\eta v_\chi}{2M_N} y_1 y'_2 + y_1 y'_2 M_N (\mathcal{F}_1 + \omega \mathcal{F}_2 + \omega^2 \mathcal{F}_3) \quad (\text{C4})$$

$$(m_\nu)_{13} = -\frac{v_\eta v_\chi}{2M_N} y_1 y'_3 + y_1 y'_3 M_N (\mathcal{F}_1 + \omega^2 \mathcal{F}_2 + \omega \mathcal{F}_3) \quad (\text{C5})$$

$$(m_\nu)_{21} = -\frac{v_\eta v_\chi}{2M_N} y_2 y'_1 + y_2 y'_1 M_N (\mathcal{F}_1 + \omega \mathcal{F}_2 + \omega^2 \mathcal{F}_3) \quad (\text{C6})$$

$$(m_\nu)_{22} = -\frac{v_\eta v_\chi}{2M_N} y_2 y'_2 + y_2 y'_2 M_N (\mathcal{F}_1 + \omega^2 \mathcal{F}_2 + \omega \mathcal{F}_3) \quad (\text{C7})$$

$$(m_\nu)_{23} = -\frac{v_\eta v_\chi}{2M_N} y_2 y'_3 + y_2 y'_3 M_N (\mathcal{F}_1 + \mathcal{F}_2 + \mathcal{F}_3) \quad (\text{C8})$$

$$(m_\nu)_{31} = -\frac{v_\eta v_\chi}{2M_N} y_3 y'_1 + y_3 y'_1 M_N (\mathcal{F}_1 + \omega^2 \mathcal{F}_2 + \omega \mathcal{F}_3) \quad (\text{C9})$$

$$(m_\nu)_{32} = -\frac{v_\eta v_\chi}{2M_N} y_3 y'_2 + y_3 y'_2 M_N (\mathcal{F}_1 + \mathcal{F}_2 + \mathcal{F}_3) \quad (\text{C10})$$

$$(m_\nu)_{33} = -\frac{v_\eta v_\chi}{2M_N} y_3 y'_3 + y_3 y'_3 M_N (\mathcal{F}_1 + \omega \mathcal{F}_2 + \omega^2 \mathcal{F}_3) \quad (\text{C11})$$

[1] P. A. Zyla et al. (Particle Data Group), PTEP **2020**, 083C01 (2020).

- [2] P. Minkowski, Phys. Lett. **B67**, 421 (1977).
- [3] M. Gell-Mann, P. Ramond, and R. Slansky, Conf. Proc. **C790927**, 315 (1979), 1306.4669.
- [4] R. N. Mohapatra and G. Senjanovic, Phys. Rev. Lett. **44**, 912 (1980).
- [5] O. Sawada and A. Sugamoto, eds., *Proceedings: Workshop on the Unified Theories and the Baryon Number in the Universe: Tsukuba, Japan, February 13-14, 1979* (Natl.Lab.High Energy Phys., Tsukuba, Japan, 1979).
- [6] T. Yanagida, Prog. Theor. Phys. **64**, 1103 (1980).
- [7] J. Schechter and J. W. F. Valle, Phys. Rev. **D22**, 2227 (1980).
- [8] R. N. Mohapatra and G. Senjanovic, Phys. Rev. **D23**, 165 (1981).
- [9] G. Lazarides, Q. Shafi, and C. Wetterich, Nucl. Phys. **B181**, 287 (1981).
- [10] C. Wetterich, Nucl. Phys. **B187**, 343 (1981).
- [11] J. Schechter and J. W. F. Valle, Phys. Rev. **D25**, 774 (1982).
- [12] R. Foot, H. Lew, X. G. He, and G. C. Joshi, Z. Phys. **C44**, 441 (1989).
- [13] M. Roncadelli and D. Wyler, Phys. Lett. B **133**, 325 (1983).
- [14] P. Roy and O. U. Shanker, Phys. Rev. Lett. **52**, 713 (1984), [Erratum: Phys.Rev.Lett. 52, 2190 (1984)].
- [15] K. S. Babu and X. G. He, Mod. Phys. Lett. **A4**, 61 (1989).
- [16] J. T. Peltoniemi, D. Tommasini, and J. W. F. Valle, Phys. Lett. **B298**, 383 (1993).
- [17] S. Centelles Chuliá, E. Ma, R. Srivastava, and J. W. F. Valle, Phys. Lett. **B767**, 209 (2017), 1606.04543.
- [18] A. Aranda, C. Bonilla, S. Morisi, E. Peinado, and J. W. F. Valle, Phys. Rev. **D89**, 033001 (2014), 1307.3553.
- [19] P. Chen, G.-J. Ding, A. D. Rojas, C. A. Vaquera-Araujo, and J. W. F. Valle, JHEP **01**, 007 (2016), 1509.06683.
- [20] E. Ma, N. Pollard, R. Srivastava, and M. Zakeri, Phys. Lett. **B750**, 135 (2015), 1507.03943.
- [21] M. Reig, J. W. F. Valle, and C. A. Vaquera-Araujo, Phys. Rev. **D94**, 033012 (2016), 1606.08499.
- [22] W. Wang and Z.-L. Han (2016), [JHEP04,166(2017)], 1611.03240.
- [23] W. Wang, R. Wang, Z.-L. Han, and J.-Z. Han, Eur. Phys. J. **C77**, 889 (2017), 1705.00414.
- [24] F. Wang, W. Wang, and J. M. Yang, Europhys. Lett. **76**, 388 (2006), hep-ph/0601018.
- [25] S. Gabriel and S. Nandi, Phys. Lett. **B655**, 141 (2007), hep-ph/0610253.

- [26] S. M. Davidson and H. E. Logan, Phys. Rev. **D80**, 095008 (2009), 0906.3335.
- [27] S. M. Davidson and H. E. Logan, Phys. Rev. **D82**, 115031 (2010), 1009.4413.
- [28] C. Bonilla and J. W. F. Valle, Phys. Lett. **B762**, 162 (2016), 1605.08362.
- [29] Y. Farzan and E. Ma, Phys. Rev. **D86**, 033007 (2012), 1204.4890.
- [30] C. Bonilla, E. Ma, E. Peinado, and J. W. F. Valle, Phys. Lett. **B762**, 214 (2016), 1607.03931.
- [31] E. Ma and O. Popov, Phys. Lett. **B764**, 142 (2017), 1609.02538.
- [32] E. Ma and U. Sarkar, Phys. Lett. **B776**, 54 (2018), 1707.07698.
- [33] D. Borah, Phys. Rev. **D94**, 075024 (2016), 1607.00244.
- [34] D. Borah and A. Dasgupta, JCAP **1612**, 034 (2016), 1608.03872.
- [35] D. Borah and A. Dasgupta, JHEP **01**, 072 (2017), 1609.04236.
- [36] D. Borah and A. Dasgupta, JCAP **1706**, 003 (2017), 1702.02877.
- [37] S. Centelles Chuliá, R. Srivastava, and J. W. F. Valle, Phys. Lett. **B773**, 26 (2017), 1706.00210.
- [38] C. Bonilla, J. M. Lamprea, E. Peinado, and J. W. F. Valle, Phys. Lett. **B779**, 257 (2018), 1710.06498.
- [39] N. Memenga, W. Rodejohann, and H. Zhang, Phys. Rev. **D87**, 053021 (2013), 1301.2963.
- [40] D. Borah and B. Karmakar, Phys. Lett. **B780**, 461 (2018), 1712.06407.
- [41] S. Centelles Chuliá, R. Srivastava, and J. W. F. Valle, Phys. Lett. **B781**, 122 (2018), 1802.05722.
- [42] S. Centelles Chuliá, R. Srivastava, and J. W. F. Valle (2018), 1804.03181.
- [43] Z.-L. Han and W. Wang (2018), 1805.02025.
- [44] D. Borah, B. Karmakar, and D. Nanda, JCAP **1807**, 039 (2018), 1805.11115.
- [45] D. Borah and B. Karmakar, Phys. Lett. **B789**, 59 (2019), 1806.10685.
- [46] D. Borah, D. Nanda, and A. K. Saha (2019), 1904.04840.
- [47] S. Centelles Chuliá, R. Cepedello, E. Peinado, and R. Srivastava, JHEP **10**, 093 (2019), 1907.08630.
- [48] S. Jana, V. P. K., and S. Saad (2019), 1910.09537.
- [49] D. Nanda and D. Borah (2019), 1911.04703.
- [50] S.-Y. Guo and Z.-L. Han, JHEP **12**, 062 (2020), 2005.08287.
- [51] N. Bernal, J. Calle, and D. Restrepo, Phys. Rev. D **103**, 095032 (2021), 2102.06211.
- [52] D. Borah, S. Mahapatra, D. Nanda, and N. Sahu, Phys. Lett. B **833**, 137297 (2022),

2204.08266.

- [53] S.-P. Li, X.-Q. Li, X.-S. Yan, and Y.-D. Yang, *Eur. Phys. J. C* **82**, 1078 (2022), 2204.09201.
- [54] M. Dey and S. Roy (2024), 2403.12461.
- [55] L. Singh, M. Kashav, and S. Verma (2024), 2405.07165.
- [56] F. Zwicky, *Helv. Phys. Acta* **6**, 110 (1933), [Gen. Rel. Grav.41,207(2009)].
- [57] V. C. Rubin and W. K. Ford, Jr., *Astrophys. J.* **159**, 379 (1970).
- [58] D. Clowe, M. Bradac, A. H. Gonzalez, M. Markevitch, S. W. Randall, C. Jones, and D. Zaritsky, *Astrophys. J.* **648**, L109 (2006), astro-ph/0608407.
- [59] N. Aghanim et al. (Planck), *Astron. Astrophys.* **641**, A6 (2020), [Erratum: *Astron. Astrophys.* 652, C4 (2021)], 1807.06209.
- [60] J. Aalbers et al. (LUX-ZEPLIN) (2022), 2207.03764.
- [61] G. Arcadi, M. Dutra, P. Ghosh, M. Lindner, Y. Mambrini, M. Pierre, S. Profumo, and F. S. Queiroz (2017), 1703.07364.
- [62] N. Bernal, M. Heikinheimo, T. Tenkanen, K. Tuominen, and V. Vaskonen, *Int. J. Mod. Phys. A* **32**, 1730023 (2017), 1706.07442.
- [63] G. Altarelli and F. Feruglio, *Rev. Mod. Phys.* **82**, 2701 (2010), 1002.0211.
- [64] S. F. King and C. Luhn, *Rept. Prog. Phys.* **76**, 056201 (2013), 1301.1340.
- [65] S. T. Petcov, *Eur. Phys. J. C* **78**, 709 (2018), 1711.10806.
- [66] G. Chauhan, P. S. B. Dev, I. Dubovyk, B. Dziewit, W. Flieger, K. Grzanka, J. Gluza, B. Karmakar, and S. Zieba (2023), 2310.20681.
- [67] G.-J. Ding and J. W. F. Valle (2024), 2402.16963.
- [68] M. Hirsch, S. Morisi, E. Peinado, and J. W. F. Valle, *Phys. Rev. D* **82**, 116003 (2010), 1007.0871.
- [69] D. Meloni, S. Morisi, and E. Peinado, *Phys. Lett. B* **697**, 339 (2011), 1011.1371.
- [70] M. S. Boucenna, M. Hirsch, S. Morisi, E. Peinado, M. Taoso, and J. W. F. Valle, *JHEP* **05**, 037 (2011), 1101.2874.
- [71] A. Adulpravitchai, B. Batell, and J. Pradler, *Phys. Lett. B* **700**, 207 (2011), 1103.3053.
- [72] D. A. Eby and P. H. Frampton, *Phys. Lett. B* **713**, 249 (2012), 1111.4938.
- [73] M. S. Boucenna, S. Morisi, E. Peinado, Y. Shimizu, and J. W. F. Valle, *Phys. Rev. D* **86**, 073008 (2012), 1204.4733.
- [74] Y. Hamada, T. Kobayashi, A. Ogasahara, Y. Omura, F. Takayama, and D. Yasuhara, *JHEP*

- 10**, 183 (2014), 1405.3592.
- [75] J. M. Lamprea and E. Peinado, Phys. Rev. D **94**, 055007 (2016), 1603.02190.
- [76] L. M. G. De La Vega, R. Ferro-Hernandez, and E. Peinado, Phys. Rev. D **99**, 055044 (2019), 1811.10619.
- [77] J. Ganguly, J. Gluza, and B. Karmakar, JHEP **11**, 074 (2022), 2209.08610.
- [78] C. Bonilla, J. Herms, O. Medina, and E. Peinado, JHEP **06**, 078 (2023), 2301.10811.
- [79] J. Ganguly, J. Gluza, B. Karmakar, and S. Mahapatra (2023), 2311.15997.
- [80] R. Kumar, N. Nath, and R. Srivastava (2024), 2406.00188.
- [81] K. Abazajian et al. (2019), 1907.04473.
- [82] B. A. Benson et al. (SPT-3G), Proc. SPIE Int. Soc. Opt. Eng. **9153**, 91531P (2014), 1407.2973.
- [83] P. Ade et al. (Simons Observatory), JCAP **02**, 056 (2019), 1808.07445.
- [84] S. Aiola et al. (CMB-HD) (2022), 2203.05728.
- [85] P.-H. Gu and U. Sarkar, Phys. Rev. D **77**, 105031 (2008), 0712.2933.
- [86] E. Ma (2019), 1905.01535.
- [87] E. Ma, Phys. Lett. B **793**, 411 (2019), 1901.09091.
- [88] E. Ma, Phys. Lett. B **809**, 135736 (2020), 1912.11950.
- [89] J. Leite, A. Morales, J. W. F. Valle, and C. A. Vaquera-Araujo, Phys. Lett. B **807**, 135537 (2020), 2003.02950.
- [90] T. A. Chowdhury, M. Ehsanuzzaman, and S. Saad, JCAP **08**, 076 (2022), 2203.14983.
- [91] D. Borah, E. Ma, and D. Nanda, Phys. Lett. B **835**, 137539 (2022), 2204.13205.
- [92] D. Borah, P. Das, and D. Nanda, Eur. Phys. J. C **84**, 140 (2024), 2211.13168.
- [93] I. Esteban, M. Gonzalez-Garcia, M. Maltoni, T. Schwetz, and A. Zhou, JHEP **09**, 178 (2020), 2007.14792.
- [94] P. F. de Salas, D. V. Forero, S. Gariazzo, P. Martínez-Miravé, O. Mena, C. A. Ternes, M. Tórtola, and J. W. F. Valle, JHEP **02**, 071 (2021), 2006.11237.
- [95] A. Ahriche, A. Jueid, and S. Nasri, Phys. Rev. **D97**, 095012 (2018), 1710.03824.
- [96] D. Borah, D. Nanda, N. Narendra, and N. Sahu, Nucl. Phys. B **950**, 114841 (2020), 1810.12920.
- [97] D. Mahanta and D. Borah, JCAP **11**, 021 (2019), 1906.03577.
- [98] G. Alguero, G. Belanger, F. Boudjema, S. Chakraborti, A. Goudelis, S. Kraml, A. Mjallal,

- and A. Pukhov, *Comput. Phys. Commun.* **299**, 109133 (2024), 2312.14894.
- [99] A. Semenov, *Comput. Phys. Commun.* **201**, 167 (2016), 1412.5016.
- [100] A. H. Abdelhameed et al. (CRESST), *Phys. Rev. D* **100**, 102002 (2019), 1904.00498.
- [101] P. Agnes et al. (DarkSide), *Phys. Rev. Lett.* **121**, 081307 (2018), 1802.06994.
- [102] J. Aalbers et al. (DARWIN), *JCAP* **11**, 017 (2016), 1606.07001.
- [103] R. H. Cyburt, B. D. Fields, K. A. Olive, and T.-H. Yeh, *Rev. Mod. Phys.* **88**, 015004 (2016), 1505.01076.
- [104] A. G. Adame et al. (DESI) (2024), 2404.03002.
- [105] G. Mangano, G. Miele, S. Pastor, T. Pinto, O. Pisanti, and P. D. Serpico, *Nucl. Phys. B* **729**, 221 (2005), hep-ph/0506164.
- [106] E. Grohs, G. M. Fuller, C. T. Kishimoto, M. W. Paris, and A. Vlasenko, *Phys. Rev. D* **93**, 083522 (2016), 1512.02205.
- [107] P. F. de Salas and S. Pastor, *JCAP* **1607**, 051 (2016), 1606.06986.
- [108] K. N. Abazajian and J. Heeck, *Phys. Rev.* **D100**, 075027 (2019), 1908.03286.
- [109] P. Fileviez Pérez, C. Murgui, and A. D. Plascencia, *Phys. Rev.* **D100**, 035041 (2019), 1905.06344.
- [110] C. Han, M. López-Ibáñez, B. Peng, and J. M. Yang (2020), 2001.04078.
- [111] X. Luo, W. Rodejohann, and X.-J. Xu, *JCAP* **06**, 058 (2020), 2005.01629.
- [112] D. Borah, A. Dasgupta, C. Majumdar, and D. Nanda, *Phys. Rev. D* **102**, 035025 (2020), 2005.02343.
- [113] P. Adshead, Y. Cui, A. J. Long, and M. Shamma (2020), 2009.07852.
- [114] X. Luo, W. Rodejohann, and X.-J. Xu (2020), 2011.13059.
- [115] D. Mahanta and D. Borah (2021), 2101.02092.
- [116] Y. Du and J.-H. Yu (2021), 2101.10475.
- [117] A. Biswas, D. Borah, and D. Nanda (2021), 2103.05648.
- [118] S.-P. Li, X.-Q. Li, X.-S. Yan, and Y.-D. Yang, *Chin. Phys. C* **47**, 043109 (2023), 2202.10250.
- [119] N. Das and D. Borah, *Phys. Rev. D* **109**, 075045 (2024), 2312.06777.
- [120] A. Biswas, D. Borah, N. Das, and D. Nanda, *Phys. Rev. D* **107**, 015015 (2023), 2205.01144.
- [121] Y. Kuno and Y. Okada, *Rev. Mod. Phys.* **73**, 151 (2001), hep-ph/9909265.
- [122] K. Afanaciev et al. (MEG II), *Eur. Phys. J. C* **84**, 216 (2024), 2310.12614.
- [123] G. Aad et al. (ATLAS), *JHEP* **08**, 104 (2022), 2202.07953.

- [124] M. Gustafsson, S. Rydbeck, L. Lopez-Honorez, and E. Lundstrom, Phys. Rev. **D86**, 075019 (2012), 1206.6316.
- [125] A. Datta, N. Ganguly, N. Khan, and S. Rakshit, Phys. Rev. **D95**, 015017 (2017), 1610.00648.
- [126] P. Poullose, S. Sahoo, and K. Sridhar, Phys. Lett. **B765**, 300 (2017), 1604.03045.
- [127] M. Hashemi and S. Najjari (2016), 1611.07827.
- [128] A. Belyaev, G. Cacciapaglia, I. P. Ivanov, F. Rojas, and M. Thomas (2016), 1612.00511.
- [129] A. Belyaev, T. R. Fernandez Perez Tomei, P. G. Mercadante, C. S. Moon, S. Moretti, S. F. Novaes, L. Panizzi, F. Rojas, and M. Thomas, Phys. Rev. D **99**, 015011 (2019), 1809.00933.
- [130] A. M. Sirunyan et al. (CMS), JHEP **07**, 027 (2021), 2103.06956.
- [131] B. Barman, D. Borah, A. Dasgupta, and A. Ghoshal, Phys. Rev. D **106**, 015007 (2022), 2205.03422.
- [132] B. Barman, D. Borah, S. Jyoti Das, and I. Saha, JCAP **10**, 053 (2023), 2307.00656.
- [133] G. B. Gelmini, S. Pascoli, E. Vitagliano, and Y.-L. Zhou, JCAP **02**, 032 (2021), 2009.01903.
- [134] S. F. King, R. Roshan, X. Wang, G. White, and M. Yamazaki, Phys. Rev. D **109**, 024057 (2024), 2308.03724.
- [135] D. Borah, N. Das, and R. Roshan (2024), 2406.04404.
- [136] X.-G. He, Y.-Y. Keum, and R. R. Volkas, JHEP **04**, 039 (2006), hep-ph/0601001.